Hyperfine Interact (2011) 203:75–84
DOI 10.1007/s10751-011-0349-x

Synthesis and characterization of Cu^{2+} substituted magnetite

A. L. Morales · A. A. Velásquez · J. P. Urquijo · E. Baggio

Published online: 25 August 2011

Abstract Samples of magnetite, both pure and doped with divalent copper, $Fe_{3-x}Cu_xO_4$, with $x = 0, 0.05, 0.10$ and 0.20 atm.%, were synthesized hydrothermally. The samples were characterized by Atomic Absorption Spectroscopy, Mössbauer Spectroscopy, X-ray diffraction, Scanning Electron Microscopy and SQUID magnetometry. The analyses made by the above techniques showed that as the Cu^{2+} concentration increases, a simultaneous reduction in the magnetic and structural parameters takes place, namely: magnetic hyperfine interactions at octahedral sites, particle size and lattice constant. Degradation in the particles morphology as well as a distribution of their size were also observed. Our study points two important effects of Cu^{2+} in magnetite, the first one is its incorporation within the structure, replacing Fe^{2+} ions and decreasing both the magnetic hyperfine interactions at octahedral sites and the bulk magnetization, the second one is the contraction of the crystalline lattice of magnetite, because incorporation of Cu^{2+} within the structure, generation of vacancies or both simultaneous effects.

Keywords Magnetite · Divalent copper · Mössbauer spectroscopy · Morphology · SQUID magnetometry

A. L. Morales · J. P. Urquijo
Grupo de Estado Sólido, Instituto de Física, Universidad de Antioquia,
A.A. 1226, Medellín, Colombia

A. A. Velásquez (✉)
Grupo de Electromagnetismo Aplicado, Universidad EAFIT,
A.A. 3300, Medellín, Colombia
e-mail: avelas26@eafit.edu.co

E. Baggio
Centro Brasileiro de Pesquisas Físicas, CEP 22290-180,
Rio de Janeiro, Brasil

1 Introduction

Magnetite is an iron oxide present on the surface of ancient rocks, as well as in the rust formed on the surfaces of iron and steel exposed to atmospheric conditions [1–3]. In the last decades some investigations [4–6] had as main objective understanding how changes in magnetic, electrical and structural properties occur when magnetite is synthesized in presence of cations such as Al^{3+}, Co^{2+}, Cr^{3+}, Mn^{2+}, Ti^{4+}, Cu^{2+}, among others. The reason for this interest is that magnetite doped with these cations can acquire properties that it does not have in its non doped form, for example, thermal conductivity variations, electrical conductivity, crystalline structure, morphology and particles size, oxidation stability, among others. In particular, the research on the effects of copper in magnetite has two paths: the first one deals with the formation of magnetite in presence of Cu^{2+}, where copper ions can prevent the formation of other iron oxides; the second and more fundamental one deals with the substitution Fe^{2+} by Cu^{2+} and also with the consequences this has for magnetite properties. In this paper we present the results obtained from the synthesis of magnetite in presence of Cu^{2+} in different atomic concentrations, looking for a fundamental approach to the mechanism by which this cation introduces changes in structural and magnetic properties of this iron oxide.

2 Experimental procedure

The samples were synthesized by the hydrothermal method reported by Schwertmann and Cornell [7]. $FeCl_2$–$4H_2O$ was used as Fe^{2+} precursor and $NaNO_3$ was used as Fe^{2+} oxidant. Non doped magnetite was synthesized from 0.1 M (300 ml) $FeCl_2$–$4H_2O$ aqueous solution, which was constantly bubbled with $N_{2(g)}$ and heated in a thermal bath at 90°C. During a 5 min period 100 ml of an alkaline mixture composed of NaOH 3 M and $NaNO_3$ 0.06 M were added dropwise to the before solution. After that, the reaction continued at 90°C during 30 min with vigorous stirring. The black precipitate was repeatedly washed with deionized water to obtain a neutral pH in the residual supernatant. Finally the precipitate was filtered and dried in an oven at 40°C for 48 h. The doped magnetites were prepared from 300 ml of aqueous solutions 0.1 M in $FeCl_2$–$4H_2O$ and 1.662×10^{-3} M, 3.324×10^{-3} M and 6.648×10^{-3} M in $CuCl_2$–$2H_2O$ for 5, 10 and 20 atm.%-Cu^{2+}, respectively. The subsequent procedure was the same described for the non doped magnetite.

Atomic Absorption Spectroscopy measurements were made with an UNICAM 929 AA Spectrometer with copper lamp, the samples were diluted in HCl solutions for these measurements. X-ray diffraction patterns were taken with a FreibergerPrazisiosmechanik Zeiss HZG-4 powder diffractometer with copper anode and wavelength of 1.5406 Å, angular step of 0.05° and sweep velocity of 1 s/step. SEM images were taken with a Low Vacuum Scanning Electron Microscopy JEOL model JSM-6460LV, operating at voltages of 20 kV and magnifications up to ×40,000. Mössbauer spectra were taken with a Wissel Spectrometer model MR260 with ^{57}Co (Rh) radioactive source, 512 channels and triangular velocity waveform. Magnetization measurements at 300 K were taken with a Quantum Design MPSM series XL SQUID magnetometer.

Table 1 Weight percentage of copper found in the samples by atomic absorption spectroscopy

Sample	Measured copper concentration (%wt)	Expected copper concentration (%wt)
mag0cu	Non doped	Non doped
mag5cu	1.14 ± 0.02	1.62
mag10cu	2.32 ± 0.04	3.24
mag20cu	4.78 ± 0.09	6.48

3 Results and discussion

3.1 Atomic absorption analyses

The Table 1 shows the weight percentages of copper measured in the different samples, as well as the expected copper concentrations calculated from the initial solutions prepared. According to the doping percentage, the samples were labeled: mag0cu, mag5cu, mag10cu and mag20cu for $x = 0$, 5, 10 and 20 atm.%-Cu^{2+} respectively.

It can be observed that the copper concentration measured in the samples increases as the copper content increases in the synthesis process, being the weight percentage of copper close to 70% of the initial copper present in the synthesis of each doped sample.

3.2 XRD measurements

X-ray diffraction patterns of the samples are presented in Fig. 1. Only peaks of magnetite were found in all cases. The Table 2 shows the structural and spectral parameters of the samples obtained by Rietveld analysis [8]. Lattice parameter of the samples decreases as the Cu^{2+} content increases, this behavior can be seen from the shifting of the principal peak $\boldsymbol{(2\theta_{311})}$ to higher angles. Due to the ionic radius of Cu^{2+} (0.69 Å) is smaller than that of Fe^{2+} (0.76 Å) a contraction of the crystalline lattice is expected as a consequence of Fe^{2+} by Cu^{2+} substitution. The mean crystallite diameter (MCD) decreases as Cu^{2+} content increases, which is consistent with the increasing value of the FWHM parameter for the principal peak, both tendencies show that the presence of Cu^{2+} in the solution also interferes with the growth of magnetite crystals.

3.3 SEM measurements

SEM analyses of the samples are shown in Fig. 2 and Table 3. The sample mag0cu consists of nearly cubic particles of well defined planes and edges, with a particle size distribution ranging from 100 to 200 nm. In the sample mag5cu the mean particle size decreases to 120 nm, keeping a cubic shape. In the samples mag10cu and mag20cu, particles without a definite shape are observed, whose sizes are close to 80 and 50 nm, respectively.

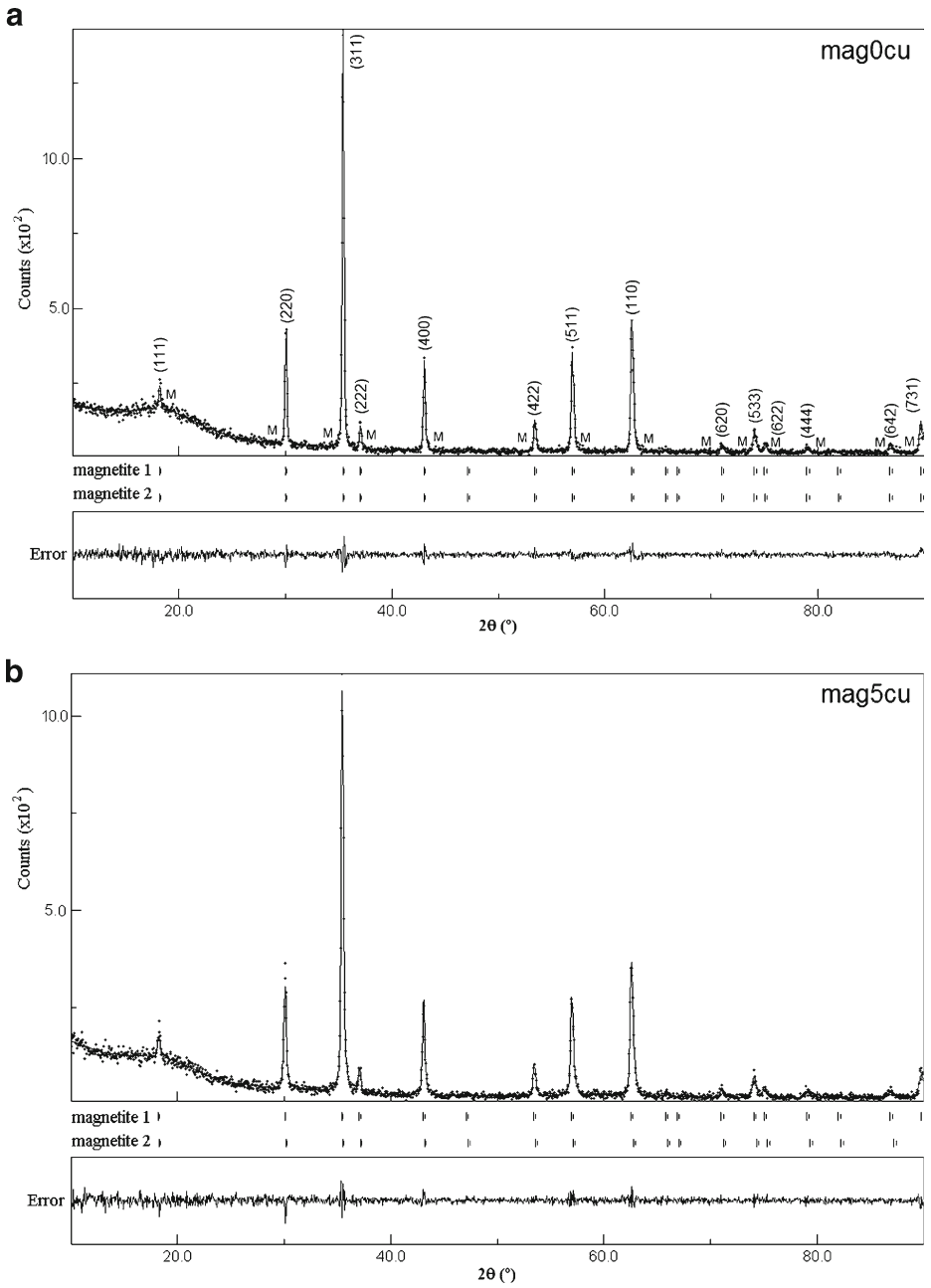

Fig. 1 X-Ray patterns of the samples

3.4 Mössbauer spectroscopy measurements

Room temperature Mössbauer spectra of the samples are presented in Fig. 3 and the hyperfine parameters obtained by least square fitting of the spectra with the

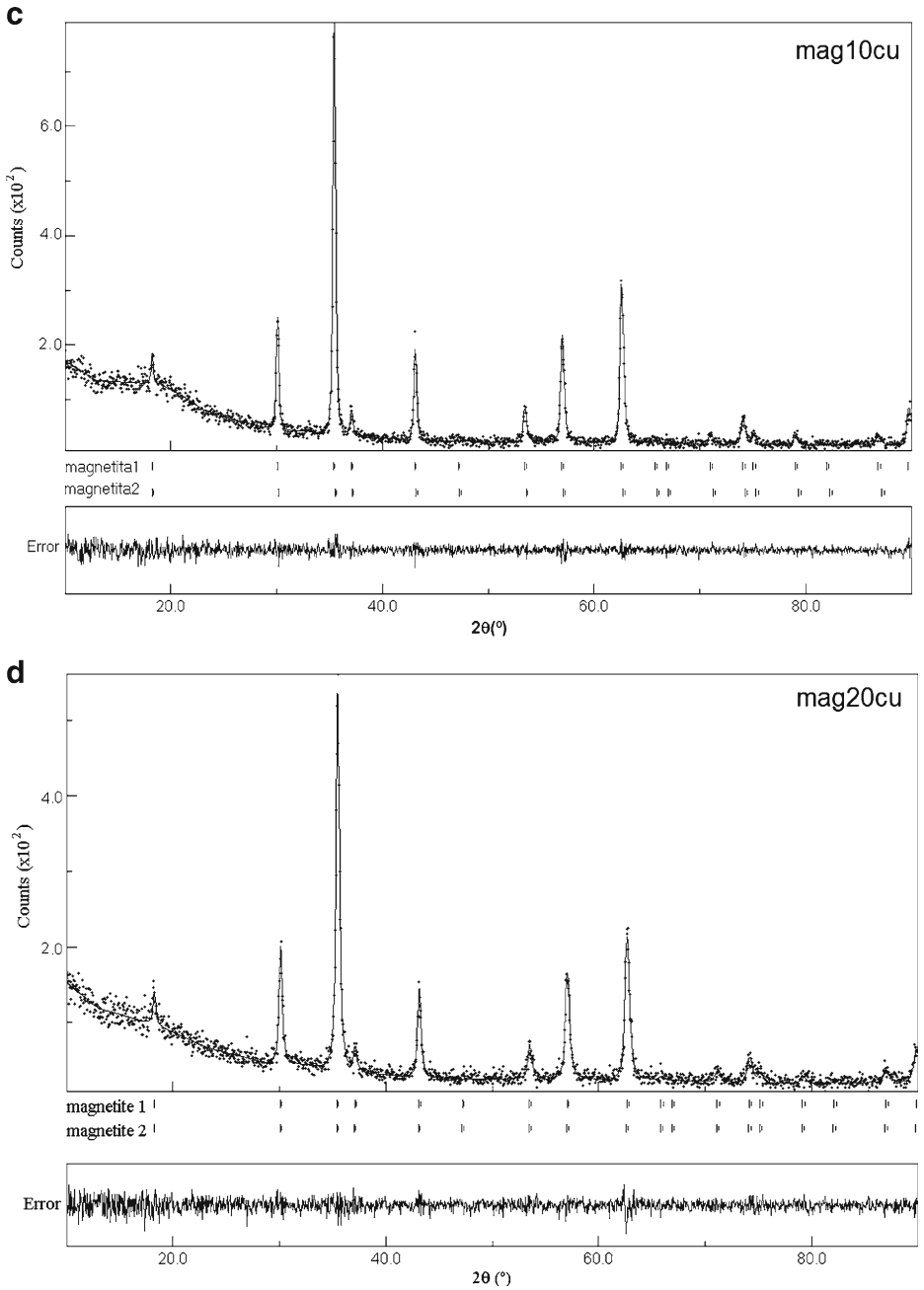

Fig. 1 (continued)

MOSF and DIST3EN software [9] are presented in Table 4. Due to the broad and asymmetrical character of the spectral lines, distributions of hyperfine magnetic fields of each spectrum were obtained first, in order to find the most probable fields

Table 2 Structural and spectral parameters of the samples obtained by Rietveld analysis

Sample	a (Å)	MCD (nm)	$2\theta_{311} \pm 0.025$	FWHM(°) ± 0.025
mag0cu	8.3852 (6)	110	35.496	0.068
mag5cu	8.3806 (6)	80	35.521	0.101
mag10cu	8.3793 (6)	80	35.550	0.118
mag20cu	8.3734 (6)	35	35.561	0.176

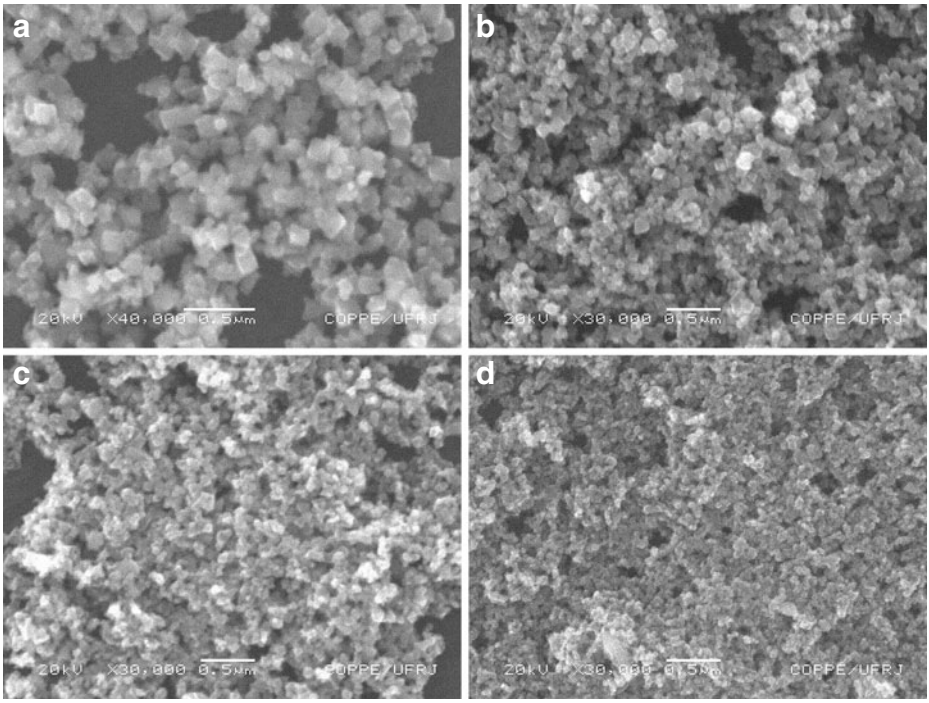

Fig. 2 SEM images of the samples

Table 3 Particle size estimated from SEM images

Sample	Particle size (nm)
mag0cu	200
mag5cu	120
mag10cu	80
mag20cu	50

of each distribution. Hyperfine magnetic field distributions are not presented here for sake of brevity.

Magnetic hyperfine field distributions of the samples mag5cu, mag10cu and mag20cu show one intermediate component of field around 45.4, 44.6 and 43.2 T, respectively. These intermediate components can be attributed to partial substitution of Fe^{2+} by Cu^{2+} at octahedral sites, due to the magnetic moment of Fe^{2+} is 4 μ_B while the magnetic moment of Cu^{2+} is 1 μ_B. A field component near to 45.8 T is present in all samples, this value is close to the hyperfine magnetic field of 46.0 T at octahedral

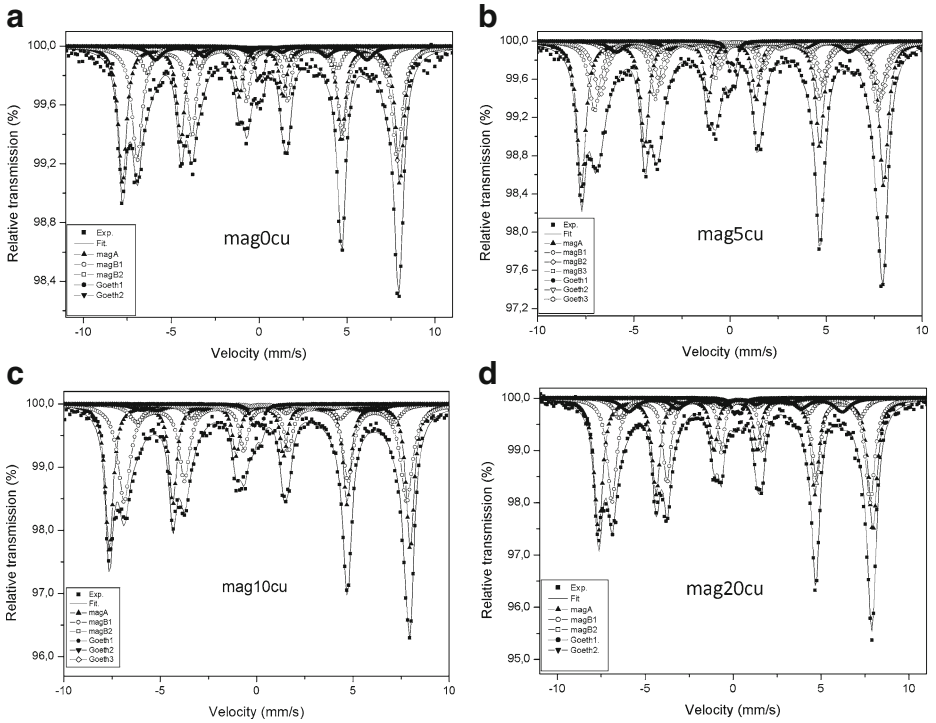

Fig. 3 Room temperature Mössbauer spectra of the samples

Table 4 Mössbauer parameters of the samples

Sample	B_{hfA} (± 0.2 T)	B_{hfB} (± 0.2 T)	IS_A (± 0.02 mm/s)	IS_B (± 0.02 mm/s)	QS_A (± 0.02 mm/s)	QS_B (± 0.02 mm/s)	$R=A(Fe^{2.5+})/A(Fe^{3+})$
mag0cu	48.8	45.8	0.23	0.57	0.00	0.00	1.31 ± 0.04
		42.1		0.60		−0.02	
mag5cu	48.7	45.7	0.24	0.47	−0.02	−0.06	1.25 ± 0.04
		45.4		0.70		−0.05	
		42.2		0.50		−0.03	
mag10cu	48.4	45.6	0.28	0.59	−0.01	−0.03	1.15 ± 0.03
		44.6		0.58		−0.04	
		41.4		0.56		−0.03	
mag20cu	48.4	45.5	0.25	0.58	0.01	−0.04	1.08 ± 0.03
		43.2		0.55		−0.02	
		42.4		0.47		−0.03	

Subscripts A and B represent tetrahedral and octahedral sites of magnetite, respectively

B_{hf} hyperfine magnetic field, *IS* isomer shift relative to α-Fe, *QS* quadrupole splitting, *R* area ratios between octahedral sub spectra and tetrahedral sub spectra

sites of a stoichiometric magnetite [2], which indicates that our samples also keep crystalline sites with properties similar to those of stoichiometric magnetite. A low field component, close to 42 T appears in all spectra, indicating that this contribution does not depend of the Cu^{2+} content used in the doping process, but it is due to the presence of vacancies or excess of Fe^{3+} in the samples. This component can be

Table 5 Mössbauer parameters of magnetic goethite impurity found in the samples

Sample	B_{hf} (±0.2 T)	IS (±0.02 mm/s)	QS (±0.02 mm/s)	W (±0.02 mm/s)	ΔW (±0.02 mm/s)	A (%)
mag0cu	37.8	0.36	−0.22	0.75	0.11	6.00 ± 0.12
mag5cu	37.5	0.36	−0.22	0.75	0.20	5.00 ± 0.10
mag10cu	37.8	0.36	−0.22	0.74	0.22	4.00 ± 0.12
mag20cu	37.7	0.36	−0.22	0.75	0.13	8.00 ± 0.16

Isomer shifts are relative to α-Fe

Table 6 Mössbauer parameters of the doublet attributed to superparamagnetic goethite impurity found in all samples

Sample	IS (±0.02 mm/s)	QS (±0.02 mm/s)	W (±0.02 mm/s)	A (%)
mag0cu	0.16	0.31	0.27	2.40 ± 0.05
mag5cu	0.23	0.32	0.26	1.90 ± 0.04
mag10cu	0.15	0.40	0.40	1.60 ± 0.03
mag20cu	0.36	0.38	0.40	1.40 ± 0.03

Isomer shifts are relative to α-Fe

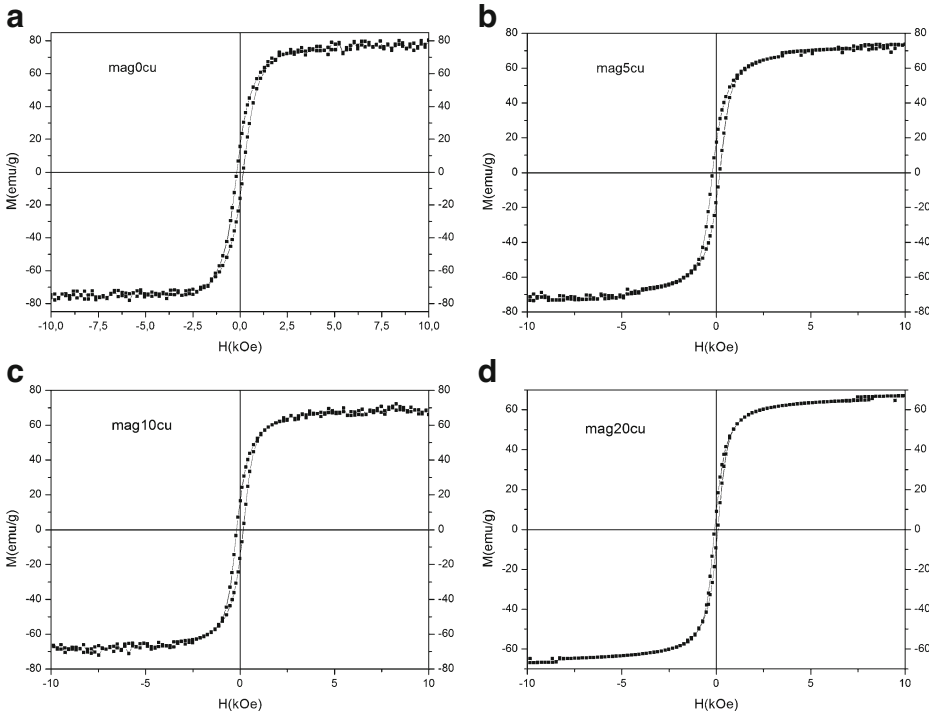

Fig. 4 Hysteresis loops of the samples

attributed to the fact that synthetic magnetite presents a high oxidation tendency, which means it can present an excess of Fe^{3+} at octahedral sites and vacancies possibly at both octahedral and tetrahedral sites. The unbalanced distribution of Fe^{2+}

Table 7 Hysteresis parameters of the samples

Sample	M_{sat}(emu/g)	M_{rem}(emu/g)	H_c(Oe)
mag0cu	77.5 ± 0.2	16.2 ± 0.2	179 ± 2
mag5cu	73.5 ± 0.1	14.4 ± 0.2	169 ± 2
mag10cu	69.7 ± 0.1	14.3 ± 0.2	164 ± 2
mag20cu	67.1 ± 0.1	7.0 ± 0.1	73 ± 2

and Fe^{3+} ions at octahedral sites leads to local atomic distributions where the Fe^{3+} ions are surrounded by different number of Fe^{2+}, Fe^{3+} ions and vacancies, producing different magnetic fields at these sites. Diamandescu [10] also reported three main peaks at octahedral sites of a magnetite with 0.342 atm.% Cu^{2+}.

All Mössbauer spectra include one sextet and one doublet, which were attributed to a small percentage of magnetic and superparamagnetic goethite, respectively. The spectral area of these two phases does not exceeded 10%. Goethite was detected in the infrared spectra of all samples by the presence of characteristic bands located at 800 and 900 cm^{-1}. The infrared spectra are not presented here for sake of brevity. This phase is poorly crystalline due to it could not be observed in the X-ray patterns. The hyperfine parameters of the goethite phase are presented in Tables 5 and 6.

3.5 Magnetization measurements

Magnetization analyses obtained by SQUID magnetometry are shown in Fig. 4 and Table 7. The samples presented hysteresis loops characteristic of multidomain systems [11]. The saturation magnetization (M_{sat}) decreases as the Cu^{2+} content increases, which is consistent with Fe^{2+} by Cu^{2+} substitution, because the magnetic moment of Cu^{2+} is 1 μ_B while that of Fe^{2+} is 4 μ_B.

4 Conclusions

We synthesized magnetite pure and magnetite in presence of Cu^{2+}. The magnetic and structural properties of the samples were changed by the presence of Cu^{2+} in the synthesis process. A weight percentage of copper, close to 70% of the value used in starting solutions was found in the final products. Both lattice parameter and particle size decreased as Cu^{2+} content increases, which is consistent with incorporation of Cu^{2+} within the structure of magnetite, vacancy generation at crystalline sites promoted by Cu^{2+} or both simultaneous effects. From our analyses we may not know what effect is the dominant one. Morphology of the particles was also degraded, starting from cubic shape in non doped and 5 atm.%-Cu^{2+} samples to undefined shape for 10 and 20 atm.%-Cu^{2+} doped samples. Magnetic hyperfine interactions measured by Mössbauer spectroscopy showed that Cu^{2+} has an appreciable effect on the magnetic hyperfine field of the octahedral sites, creating magnetic fields lower than those of a stoichiometric magnetite, as well as broad and asymmetric lines in the octahedral sub spectra, which is consistent with substitution of Fe^{2+} by Cu^{2+}, generation of vacancies or both simultaneous effects. Saturation magnetization and coercivity also were reduced due to the lower magnetic moment of Cu^{2+} with respect to Fe^{2+}. Our study may give important elements to the understanding of the changes in magnetic and structural properties of magnetite doped with metallic cations, which

can be used to synthesize magnetite samples useful for industrial and technological applications.

References

1. Dorigueto, A.C., Fernandes, N.G., Persiano, A.L.C., Greneche, J.M.: Characterization of a natural magnetite. Phys. Chem. Miner. **30**, 250 (2003)
2. Vandenberghe, R.E.: Mössbauer spectroscopy and applications in geology. International training centre for post-graduate soil scientists, p. 25. State University Gent, Belgium (1990)
3. García, K.E., Morales, A.L., Barrero, C.A., Greneche, J.M. : New contributions to the understanding of rust layer formation in steels exposed to a total immersion test. Corrosion Sci. **48**, 2813–2830 (2006)
4. Ishikawa, T., Nakazaki, H., Yasukawa, A., Kandori, K., Seto, M.: Influences of Co^{2+}, Cu^{2+} and Cr^{3+} ions on the formation of magnetite. Corrosion Sci. **41**, 1670 (1999)
5. Pourroy, G., Valles-Minguez, A., Dintzer, T., Richard-Plouet, M.: Synthesis of Cu°/Cu(II) substituted magnetite nanocomposites in aqueous media. J. Alloys Compd. **327**, 267–269 (2001)
6. Cvejic, Z., Antic, B., Kremenovic, A., Rakic, S., Goya, G.F., Rechenberg, H.R., Jovalekic, C., Spasojevic, V.: Influence of heavy rare earth ions substitution on microstructure and magnetism of nanocrystalline magnetite. J. Alloy. Comp. **472**, 571–575 (2009)
7. Cornell, R.M., Schwertmann, U.: The iron oxides, pp. 130, 135. VCH mbH, Weinheim, Germany (1996)
8. Lutterotti, L.: Maud-Materials Analysis Using Diffraction-tutorial. http://www.ing.unitn.it/~maud/tutorial.html. Accessed 10 February 2010.
9. Vandenberghe, R., De Grave, E., De Bakker, P.M.A.: On the methodology of the analysis of Mössbauer spectra. Hyperfine Interact. **83**, 29–49 (1994)
10. Diamandescu, L., Tarabasanu-Mihaila, D., Teodorescu, V., Popescu-Pogrion, N.: Hydrothermal synthesis and structural characterization of some substituted magnetites. Mater. Lett. **37**, 340–348 (1998)
11. Khollam, Y.B., Dhage, S.R., Potdar, H.S., Deshpande, S.B., Bakare, P.P., Kulkarni, S.D., Date, S.K.: Microwave hydrothermal preparation of submicron-sized spherical magnetite (Fe_3O_4) powders. Mater. Lett. **56**, 571–577 (2002)